Measurement-Based Entanglement under Conditions of Extreme Photon Loss

Earl T. Campbell[1] and Simon C. Benjamin[1,2,*]

[1]*Department of Materials, University of Oxford, Parks Road, Oxford OX1 3PH, United Kingdom*

[2]*Centre for Quantum Technologies, National University of Singapore, 3 Science Drive 2, Singapore 117543, Singapore*

(Received 23 April 2008; published 24 September 2008)

The act of measuring optical emissions from two remote qubits can entangle them. By demanding that a photon from each qubit reaches the detectors, one can ensure that no photon was lost. But retaining both photons is rare when loss rates are high, as in Moehring *et al.* where 30 successes occurred per 10^9 attempts. We describe a means to exploit the low grade entanglement heralded by the detection of a lone photon: A subsequent perfect operation is quickly achieved by consuming this noisy resource. We require only two qubits per node, and can tolerate both path length variation and loss asymmetry. The impact of photon loss upon the failure rate is then linear; realistic high-loss devices can gain orders of magnitude in performance and thus support quantum computing.

DOI: 10.1103/PhysRevLett.101.130502 PACS numbers: 03.67.Bg, 03.67.Lx, 03.67.Pp

Using optical measurements to induce entanglement may enable scalable technologies. But photon loss can corrupt entanglement. Unfortunately detectors and routers are lossy, and sources may need filtering [diamond nitrogen-vacancy (NV) centres emit fewer than 4% of photons cleanly, without giving rise to phonons [1]].

An early solution to this problem was *weak excitation* [2–4], and this approach has been implemented experimentally with atomic ensembles [5]. Its drawback is that fidelity is inversely linked to the rate of success. Alternate *two-photon* schemes excite a photon from each source and require that both be detected [6–11], reducing the rate of success to a quadratic dependence on photon capture. Entanglement of macroscopically separate atoms was accomplished this way [12] with 30 successes in 10^9 attempts (and a new report describes a 13-fold improvement [13]).

Here we describe an approach that can be fundamentally more rapid. We generate high fidelity entanglement using lone detector "click" events, even in the limit of extreme photon loss where each click leaves the source qubits in a severely mixed state. The chosen operation is a parity projection which supports universal quantum computing via the graph state paradigm [see Fig. 1(b)]. The approach requires two qubits at each local site, a modest level of complexity that has already been demonstrated in several systems [14,15].

In order to provide a clear exposition, we will assume the specific energy level structure shown in Fig. 1. Alternatives such as Λ structures can be equally suitable. We begin by preparing each of the optically active qubits, which are termed *brokers* following Ref. [17], in state

$$|\theta\rangle = \cos(\theta)|0\rangle + \sin(\theta)|e\rangle. \quad (1)$$

Here $|e\rangle$ is the state that decays radiatively to $|1\rangle$ (see Fig. 1). We collect photons using a lens or a cavity system and direct them through a beam splitter. Given an ideal apparatus, if exactly one photon is detected then the brokers are projected onto the $(|01\rangle + |10\rangle)/\sqrt{2}$ state (neglecting any phase that depends on *which* detector clicked, which is trivially corrected by a local operation). In reality we may have non-number resolving detectors, photon loss (possibly asymmetric), and path length variations. A click then corresponds to a mixed state

$$\rho_B = (1-\eta)\mathcal{Z}_{B1}^{\phi,\Delta}|\Psi^+\rangle\langle\Psi^+|\mathcal{Z}_{B1}^{\phi,-\Delta} + \eta|11\rangle\langle 11|, \quad (2)$$

where operator $\mathcal{Z}_{B1}^{\phi,\Delta}$ represents the effects of asymmetry in the apparatus, as parameterized in Fig. 1. This operator can be formally represented as acting on broker qubit $B1$ alone:

$$\mathcal{Z}_{B1}^{\phi,\Delta} = [\cos(\phi)\mathbb{1} + \sin(\phi)Z_{B1}][\cos(\Delta)\mathbb{1} + i\sin(\Delta)Z_{B1}]. \quad (3)$$

The probability that we indeed see a click, i.e., that we obtain ρ_B from initial state $|\theta\rangle|\theta\rangle$, is [18]

$$P_{\text{click}} = T\sin^2(\theta)[2 - T\sin^2(\theta)\cos^2(2\phi)], \quad (4)$$

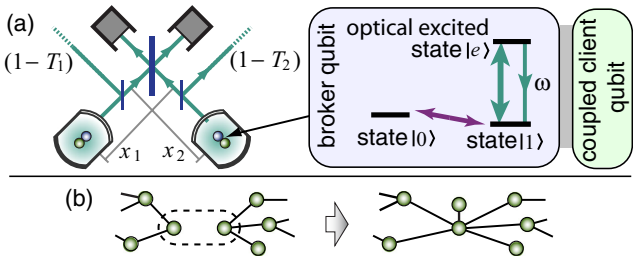

FIG. 1 (color online). (a) Schematic of an apparatus suitable for creating entanglement between distant entities, using a beam splitter for erasure of *which path* information. Our model incorporates uncertain optical path length and asymmetric photon loss via the parameters shown. Photon loss is modeled by beam splitters with transmittance T_1 and T_2; loss at different parts of the apparatus has an equivalent description in terms of T_1 and T_2. We define ϕ to be the transmittance asymmetry, such that $\sin(2\phi) = (T_1 - T_2)/(T_1 + T_2)$. Asymmetry in path length is parametrized by $\Delta = \pi(x_1 - x_2)/\lambda$. (b) A successful parity projection on a graph state [16]. The clients acted upon become entangled; prior entanglement to other clients is preserved.

where $T = (T_1 + T_2)/2$. The weighting in ρ_B is

$$\eta = \frac{\sin^2(\theta)[2 - T\cos^2(2\phi)]}{2 - T\sin^2(\theta)\cos^2(2\phi)}. \quad (5)$$

From the work of Bennett *et al.* [19] we know that there is a finite chance of distilling a perfect Bell state from any two states of the form $(1-\eta)|\Psi^+\rangle\langle\Psi^+| + \eta|11\rangle\langle 11|$. Note this is equivalent to (2) without imperfections Δ and ϕ. These noisy states have also been considered in the context of entanglement swapping in ensemble-based quantum communication, where it was found that post-selection will enable the same applications supported by a maximally entangled $|\Psi^+\rangle$ state [20]. Here we show that by successively consuming two resource states of the general form (2) we can perform a high fidelity *parity projection*.

Typical distillation protocols aim to generate a particular state [19,21,22], and detailed studies have examined the practical requirements, for example, in the communication context [23]. However, by generating a projection operation instead of a specific state, one can directly synthesize many-qubit *graph states*, the resource for measurement-based computation [16] [see Fig. 1(b)]. We find that Δ and ϕ can be completely unknown provided that they do not drift significantly over the course of the protocol, and that two qubits per node suffice for all operations.

We present our protocol in terms of a basic *routine* that must be performed more than once. The aim is to perform a single high fidelity parity projection on two remote *client* qubits, labeled Cx for local site x, which may be part of some preexisting graph state. Note that although we are adopting the *broker-client* terminology from Ref. [17], the earlier paper did not exploit the brokers for distillation and thus implicitly assumed that the initial entanglement mechanism is near perfect [$\eta \to 0$ and $\mathcal{Z} \to \mathbb{1}$ in Eq. (2)]. The first flow chart shows one routine. Note that step 2 will map $|11\rangle \to |{+}{+}\rangle$ and $\mathcal{Z}_{B1}^{\phi,\Delta}|\Psi^+\rangle \to \mathcal{X}_{B1}^{-\phi,-\Delta}|\Phi^-\rangle$, where $|\Phi^-\rangle = (|00\rangle - |11\rangle)/\sqrt{2}$, $|\pm\rangle = (|0\rangle \pm |1\rangle)/\sqrt{2}$, and $\mathcal{X}_{B1}^{\phi,\Delta}$ is analogous to $\mathcal{Z}_{B1}^{\phi,\Delta}$ with X_{B1} replacing Z_{B1}.

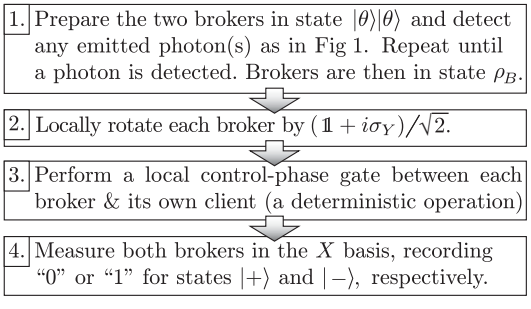

Suppose that our brokers were actually in the pure product state $|{+}{+}\rangle$ prior to steps 3 and 4. Then these steps effect a computational basis measurement on the clients, since

$$\langle i, j|H_{B1}H_{B2}\mathcal{C}_{B1}^{C1}\mathcal{C}_{B2}^{C2}|{+}{+}\rangle = S_{i,j}, \quad (6)$$

where i and j denote measurement results on the brokers, H and $\mathcal{C}$ are Hadamard and control-phase gates, and the client projector $S_{i,j} = |i, j\rangle\langle i, j|$. Alternatively, given brokers in the entangled state $\mathcal{X}_{B1}^{-\phi,-\Delta}|\Phi^-\rangle$, steps 3 and 4 will effect a parity projection while transmitting an asymmetry operator:

$$\langle i, j|H_{B1}H_{B2}\mathcal{C}_{B1}^{C1}\mathcal{C}_{B2}^{C2}\mathcal{X}_{B1}^{-\phi,-\Delta}|\Phi^-\rangle = \frac{1}{\sqrt{2}}\mathcal{Z}_{C1}^{\phi_i,\Delta_i}P_{i,j}. \quad (7)$$

Here the parity projector has opposite parity to that of i, j, so $P_{i,j} = [\mathbb{1} - (-1)^{i+j}Z_{C1}Z_{C2}]/2$, and the variables ϕ_i and Δ_i are $-(-1)^i\phi$ and $-(-1)^i\Delta$, respectively. We arrive at the full quantum operation by forming an incoherent mixture of operations (6) and (7), each weighted by their probabilities:

$$E_{i,j}(\rho_C) \equiv \tfrac{1}{2}(1-\eta)\mathcal{Z}_{C1}^{\phi_i,\Delta_i}P_{i,j}\rho_C P_{i,j}\mathcal{Z}_{C1}^{\phi_i,-\Delta_i} + \eta S_{i,j}\rho_C S_{i,j}. \quad (8)$$

Here ρ_C represents the initial state of the client qubits, which may be part of some larger graph state, e.g., Fig. 1(b). This operation is noisy, so we will need at least one more routine.

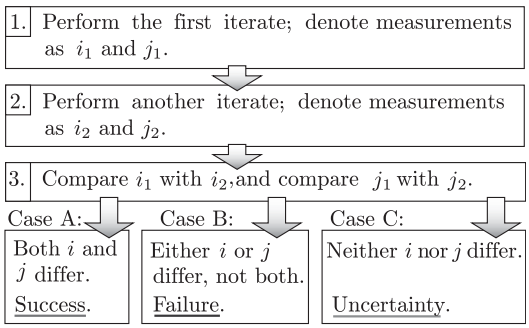

In case A we have measurement results of the same parity, but differing specific i, j values. The corresponding parity projectors are consistent, $P_{i_n,j_n}P_{i_1,j_1} = P_{i_1,j_1}$, but all other projector combinations vanish, $P_{i_n,j_n}S_{i_1,j_1} = S_{i_n,j_n}P_{i_1,j_1} = S_{i_n,j_n}S_{i_1,j_1} = 0$. We conclude with certainty that the client qubits have simply been acted on by $\mathcal{Z}_{C1}^{\phi_i,\Delta_i}\mathcal{Z}_{C1}^{-\phi_i,-\Delta_i}P_{i_1,j_1}$, which is proportional to a pure parity projection, as $\mathcal{Z}_{C1}^{\phi_i,\Delta_i}\mathcal{Z}_{C1}^{-\phi_i,-\Delta_i} = \cos(2\phi)\mathbb{1}$. This parity projection implements a fusion in the graph state picture, as shown in Fig. 1(b). The probability of reaching case A after two routines is

$$P_{\text{two}} = \cos^2(2\phi)(1-\eta)^2/2. \quad (9)$$

In case B the parity of i, j has changed and consequently $P_{i_n,j_n}P_{i_1,j_1} = 0$, so we must conclude that the client qubits have been projected into a separable state. This is an unrecoverable failure, and the clients must be reset before

trying again (any prior entanglement with other qubits is lost). In case C there is uncertainty as to which quantum operation has been performed on the clients. We could choose to abort here, declaring case C as a failure, which would be a simple "2 routines only" (2RO) strategy. Later we will show that one can also persist with further routines to resolve the uncertainty.

In Fig. 2 we characterize the performance in the simplest scenario: the client qubits have no prior entanglement and are in the trivial graph state $|+\rangle|+\rangle$. We use the 2RO protocol with broker qubits initialized in $|\theta\rangle|\theta\rangle$ to parity project the clients into Bell pairs at a rate R:

$$R(\tau^{-1}) = \frac{P_{\text{two}}}{2}\left(\frac{1}{P_{\text{click}}} + \frac{t_{\text{local}}}{\tau}\right)^{-1}. \tag{10}$$

The rate is expressed in units of $1/\tau$, where τ is the time for a single attempt at generating a photon, and t_{local} is the time taken to perform local operations for one routine. In the regime of extreme photon loss the number of optical attempts, $1/P_{\text{click}}$, will be very large. For the plots in Fig. 2 we assume that the time ratio t_{local}/τ is not comparably large so that it can be neglected. This is a fair assumption for NV centers, for example: All local operations can be implemented through electron spin manipulations, the slowest being the entangling operation which is limited by the hyperfine splitting of 10 to 100 Mhz (depending on ^{13}C location) [14,15]. Time τ can only be moderately faster, even if we neglect the time to prepare $|\theta\rangle|\theta\rangle$, due to the emission time of order 10 ns.

Rate R is optimized by a specific θ as shown in Fig. 2(a). In Fig. 2(b) we compare our approach to a two-photon entanglement scheme, finding 3 orders of magnitude improvement when T reaches 10^{-4} (the approximate value that was achieved experimentally in Ref. [12]).

Dark counts can be a primary cause of infidelity in entanglement achieved by the path-erasure approach [12]. The approach described here, with its single broker-client pair at each location, is vulnerable to accumulation of dark count noise over successive routines. However, because the number of routines is so small, the accumulation need not be substantial. To quantify the effect of dark counts and other sources of infidelity, the quality of $E(\rho_C)$ is measured by the Jamiolkowski fidelity [24]. In Fig. 2(c) we make the same comparison as in Fig. 2(b) but now with finite dark counts and insisting on a minimum fidelity of $1–10^{-3}$. If it were necessary to enter the no-go region, one could introduce further ancilla qubits and combine the protocol described here with schemes like Refs. [25–28].

Imperfect local gate operations also cause infidelity. Suppose that we are subject to general depolarizing noise: After all local rotations, the qubits at site x are depolarized with probability p_g, so that $\rho_{Bx}\rho_{Cx} \to (1 - p_g)\rho_{Bx}\rho_{Cx} + p_g \mathbb{1}/4$. Figure 3 shows how this reduces the fidelity of the final parity projection; note the dependence on the photon loss parameter η. Using the optimized θ (and hence η) for

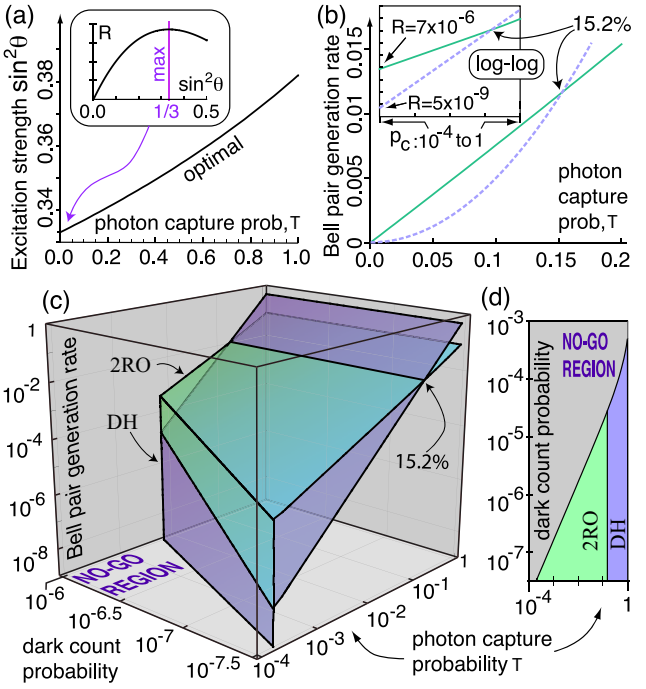

FIG. 2 (color online). Attainable rate of Bell pair production, R. (a) Optimizing experimental parameter [defined in Eq. (1)] to maximize R. (b) Linear and log-log (inset) plots comparing the rate of Bell pair production in units of $1/\tau$ using our approach (solid line) versus a comparable prior scheme, i.e., the double-heralding protocol [9] (dashed line). Other schemes involving detecting two photons [6–10] will have similar performance in the high photon loss domain. Note that the plot extends into the $T \sim 1$ regime where it may not still hold that local gate times are negligible for either protocol. If the approximation is valid for modest values of T, then we observe a crossover point at 15.2%, above which our approach is unhelpful. (c) Regions in which our approach (2RO) and double heralding (DH) have superior rates of generation, given a finite probability of a dark count occurring while we monitor for photons. Here we assume a minimum acceptable fidelity of $1–10^{-3}$; thus there is a "no-go" parameter region where both approaches fail. (d) A top-down view, over a wider range of dark counts. For simplicity we assume here that photon loss is symmetric: $T_1 = T_2 = T$.

Bell pair production under extreme photon loss, we find that the fidelity only drops by $\sim 3.5 p_g$ [see Fig. 3(b)]. Our protocol thus proves to be very robust versus local gate noise, since no protocol can achieve better than a small multiple of the local noise.

We have shown that it is not necessary to determine any difference in path length between the "arms" of the device nor any asymmetry in the transmission probabilities; the former will cancel and the later only reduces success probability without degrading the fidelity. This is valid if these quantities do not drift appreciably *during* a given instance of the protocol. Given finite drift, the infidelity is $\epsilon = (\pi D_x)^2 + (D_T/2)^2 + \text{order}(D_x, D_T)^4$ [18], which is depicted in Fig. 3(c). If only path length drift is significant,

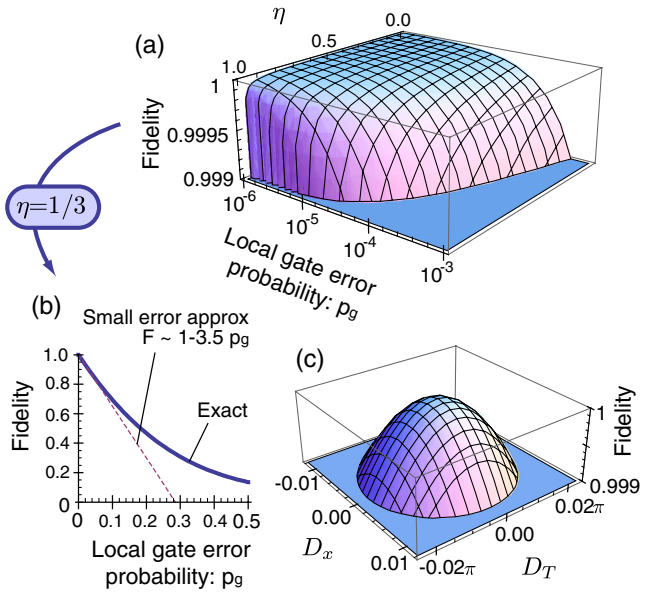

FIG. 3 (color online). The effect of various imperfections on the fidelity of our parity projection. (a) The fidelity of the 2RO strategy in the presence of imperfect local gates, plotted against local gate error probability p_g and η [18]. (b) The fidelity against local gate error probability (linear scale) for $\eta = 1/3$, which is the optimal value of η for Bell pair production under heavy photon loss. The dotted line shows the linear approximation of $F \sim 1\text{–}3.5 p_g$, which is valid for small p_g. (c) The fidelity of the 2RO strategy in the presence of drifting apparatus cut off at fidelity $1\text{–}10^{-3}$. Drift in the path length is quantified by $D_x = [(x_1 - x_2) - (x_1' - x_2')]/\lambda$, where unprimed (primed) variables represent the initial (final) values. Drift in the photon transmission probabilities is quantified by $D_T = 1 - \sqrt{(T_1' T_2')/(T_1 T_2')}$, with the same priming notation.

then the infidelity will be below 10^{-3} provided that drift $D_x < 1/(32\pi)$.

We have characterized the performance of our protocol using the specific task of generating high quality Bell pairs. But our motivation in designing a robust parity projection was to support the creation of many-qubit graph states using two-qubit nodes [see Fig. 1(b)], thus enabling universal quantum computation [16]. Through our protocol, the problem of photon loss is translated into a linear time cost (the optimum) rather than directly impacting the projection's success probability or its fidelity. Nevertheless, it is interesting to consider how one might further boost the success probability in situations where failure would be particularly damaging to the nascent graph. A simple option is to lower the value of θ, thus reducing the $|11\rangle\langle 11|$ component within ρ_B. Another route is to generalize our simple 2RO protocol so that case C need not be abandoned. In fact, this is straightforward. Over multiple routines, outright failure occurs only when the parity of measurement outcomes i, j in the latest routine differs from the previously seen parity. Success requires that all outcomes have the same parity *and* the two possible instances of that parity have occurred the *same number of times*. The latter criterion assures that any errors described by $\mathcal{Z}$ will not degrade the resulting entanglement; our former expression for the state projector simply generalizes to $(\mathcal{Z}_{C1}^{\phi_i,\Delta_i})^{n/2} \times (\mathcal{Z}_{C1}^{-\phi_i,-\Delta_i})^{n/2} P_{i_1,j_1}$, which reduces to a pure parity projection as before. Given a system where $\mathcal{Z} \to \mathbb{1}$, this criterion could of course be relaxed.

We thank Joe Fitzsimons, Sean Barrett, Jason Smith, Pieter Kok, and David Moehring for helpful comments. This research was supported by the Royal Society, the QIP IRC, and the National Research Foundation and Ministry of Education, Singapore.

*s.benjamin@qubit.org

[1] G. Davies, J. Phys. C **7**, 3797 (1974).
[2] C. Cabrillo *et al.*, Phys. Rev. A **59**, 1025 (1999).
[3] S. Bose *et al.*, Phys. Rev. Lett. **83**, 5158 (1999).
[4] D. E. Browne, M. B. Plenio, and S. F. Huelga, Phys. Rev. Lett. **91**, 067901 (2003).
[5] C. W. Chou *et al.*, Nature (London) **438**, 828 (2005).
[6] L. M. Duan and H. J. Kimble, Phys. Rev. Lett. **90**, 253601 (2003).
[7] X. L. Feng *et al.*, Phys. Rev. Lett. **90**, 217902 (2003).
[8] C. Simon and W. T. Irvine, Phys. Rev. Lett. **91**, 110405 (2003).
[9] S. D. Barrett and P. Kok, Phys. Rev. A **71**, 060310 (2005).
[10] Y. L. Lim *et al.*, Phys. Rev. Lett. **95**, 030505 (2005).
[11] S. C. Benjamin *et al.*, New J. Phys. **7**, 194 (2005).
[12] D. L. Moehring *et al.*, Nature (London) **449**, 68 (2007).
[13] D. N. Matsukevich *et al.*, Phys. Rev. Lett. **100**, 150404 (2008).
[14] M. V. Gurudev Dutt *et al.*, Science **316**, 1312 (2007).
[15] P. Neumann *et al.*, Science **320**, 1326 (2008).
[16] R. Raussendorf, D. E. Browne, and H. J. Briegel, Phys. Rev. A **68**, 022312 (2003).
[17] S. C. Benjamin *et al.*, New J. Phys. **8**, 141 (2006).
[18] See EPAPS Document No. E-PRLTAO-101-068837 for supplementary material giving technical details of the calculations made in this Letter. For more information on EPAPS, see http://www.aip.org/pubservs/epaps.html.
[19] C. H. Bennett *et al.*, Phys. Rev. A **54**, 3824 (1996).
[20] L. M. Duan *et al.*, Nature (London) **414**, 413 (2001).
[21] C. H. Bennett *et al.*, Phys. Rev. Lett. **76**, 722 (1996).
[22] D. Deutsch *et al.*, Phys. Rev. Lett. **77**, 2818 (1996).
[23] L. Childress *et al.*, Phys. Rev. A **72**, 052330 (2005).
[24] A. Gilchrist, N. K. Langford, and M. A. Nilesen, Phys. Rev. A **71**, 062310 (2005).
[25] W. Dür and H. J. Briegel, Phys. Rev. Lett. **90**, 067901 (2003).
[26] L. Jiang *et al.*, Phys. Rev. A **76**, 062323 (2007).
[27] L. M. Duan *et al.*, Quantum Inf. Comput. **4**, 165 (2004).
[28] D. K. L. Oi *et al.*, Phys. Rev. A **74**, 052313 (2006).